Real Function of Semiconducting Polymer in GaAs/Polymer Planar Heterojunction Solar Cells

Liang Yan and Wei You*

Department of Chemistry, University of North Carolina at Chapel Hill, Chapel Hill, North Carolina 27599-3290, United States

ABSTRACT We systematically investigated GaAs/polymer hybrid solar cells in a simple planar junction, aiming to fundamentally understand the function of semiconducting polymers in GaAs/polymer-based heterojunction solar cells. A library of semiconducting polymers with different band gaps and energy levels were evaluated in GaAs/polymer planar heterojunctions. The optimized thickness of the active polymer layer was discovered to be ultrathin (~10 nm). Further, the open-circuit voltage (V_{oc}) of such GaAs/polymer planar heterojunctions was fixed around 0.6 V, regardless of the HOMO energy level of the polymer employed. On the basis of this evidence and others, we conclude that n-type GaAs/polymer planar heterojunctions are *not* type II heterojunctions as originally assumed. Instead, n-type GaAs forms a Schottky barrier with its corresponding anode, while the semiconducting polymer of appropriate energy levels can function as hole transport layer and/or electron blocking layer. Additionally, we discover that both GaAs surface passivation and thermal annealing can improve the performance of GaAs/polymer hybrid solar cells.

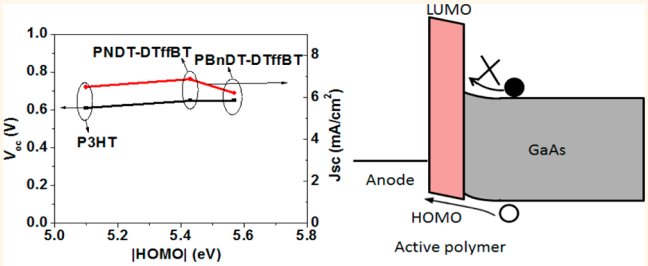

KEYWORDS: hybrid solar cell · GaAs · polymers · planar heterojunction · Schottky barrier

An organic/inorganic hybrid solar cell, if engineered properly, can combine the advantages of both organic and inorganic materials. Organic materials typically have a good light absorption coefficient (*e.g.*, requiring only a thin film), have tunable energy levels and band gaps (*e.g.*, easily matching those of inorganics), and can be processed at low cost (*e.g.*, solution processing, including roll-to-roll printing). On the other hand, inorganic materials offer high carrier mobility and good air stability. Therefore, the concept of organic/inorganic hybrid solar cells has recently gained much ground.[1−3] Studies have spanned from a variety of inorganic semiconductors, such as Si,[4−8] ZnO,[9−11] and TiO_2,[12−14] to organic materials, such as poly(3,4-ethylenedioxythiophene):poly(styrenesulfonate) (*i.e.*, PEDOT:PSS) and poly(3-hexylthiophene) (*i.e.*, P3HT). Among all these, silicon-based hybrid solar cells have reached the highest efficiency of above 10% through a planar Schottky design.[15]

Unlike Si, which has an indirect band gap, GaAs is a direct band gap material with a high light absorption coefficient and high charge carrier mobility,[16,17] both of which are excellent attributes for solar energy utilization. In fact, GaAs-based thin film solar cells have achieved a higher efficiency of 28% than that of crystalline Si (25%).[18] However, the steep price associated with high-efficiency GaAs cells also precludes their large-scale adoption. With the hope of lowering the cost and potentially higher efficiencies, GaAs-based hybrid solar cells have been attempted, although only in sporadic but notable reports.[19−25] The obtained efficiency number significantly varied. For example, while over 4% efficiencies have been obtained for a GaAs nanowire-embedded bulk heterojunction with P3HT[24] and for GaAs/oligothiophene planar junctions,[20] only 1.44% was achieved with patterned GaAs nanopillars coated with P3HT.[25] Yet in another recent report, a heterojunction between vertically aligned GaAs nanowires and PEDOT:PSS with an additional layer of P3HT showed over 9% efficiency.[22] A closer inspection and comparison of these reports revealed that the spectra−current responses in these devices

* Address correspondence to wyou@unc.edu.

Received for review December 31, 2012 and accepted July 1, 2013.

Published online July 01, 2013
10.1021/nn306047q

were noticeably different. Specifically, in both the planar heterojunction- and the patterned nanopillar-based devices, GaAs contributed significantly more to the incident photon-to-electron conversion efficiency (IPCE) spectrum than the P3HT/oligothiophene, whereas in the nanowire-embedded bulk heterojunction, the IPCE spectrum was dominated by P3HT with an almost negligible contribution from GaAs nanowires. Nevertheless, in almost all these devices, the GaAs/organics junction was unanimously *assumed* as a type II heterojunction between GaAs and thiophene-based materials (P3HT or oligothiophene), presumably based on the band alignment. This visible discrepancy in the reported IPCE spectra with almost identical materials prompted us to seek the answer to a fundamental question: *what is the real function of polymers in the GaAs/polymer-based hybrid solar cells?*

As our initial attempt to answer this question, we conducted a systematic study of a GaAs/polymer hybrid device in a planar junction (the simplest design). We chose and studied multiple polymers of different energy levels and band gaps, through optimized device fabrication conditions such as passivation, thermal annealing, and active polymer layer thickness. In the following, we will show that in the optimized devices the highest occupied molecular orbital (HOMO) of the polymer does *not* affect the open-circuit voltage (V_{oc}), as opposed to what had been predicted for a type II heterojunction. Furthermore, the short-circuit current (J_{sc}) of such planar junctions is primarily contributed by the absorption of GaAs. All these facts indicate that the polymer/n-type GaAs hybrid solar cells are actually Schottky barrier type solar cells, at least in the planar configuration. The polymer can function as hole transport layer (HTL) and electron blocking layer (EBL), if the energy levels of such a polymer are appropriately selected.

RESULT AND DISCUSSION

GaAs/P3HT. We began our investigation with regioregular P3HT, a well-studied and commercially available polymer, as our p-type model polymer, and GaAs(100) as the n-type inorganic semiconductor. We intended to use such a model system to investigate and optimize variables including surface passivation on GaAs, thickness of the active polymer layer, and thermal annealing of the active polymer layer. Figure 1 outlines the band alignment of the GaAs/P3HT/PEDOT:PSS/ITO device, indicating a likely type II heterojunction.

With the proposed type II heterojunction of GaAs/P3HT (Figure 1), there are three possible functions the active polymer (*e.g.*, P3HT) can play in the hybrid solar cell. First, the polymer can work as a hole transport layer since its HOMO is located well above the valence band of GaAs. Second, with an appropriate band gap (*e.g.*, 1.9 eV for P3HT),[26] the polymer can also absorb light to generate excited states and contribute to the photocurrent. Third, the polymers can block the electrons generated from photons absorbed by GaAs, since the LUMO energy level of the active polymer is higher than the conduction band of GaAs.

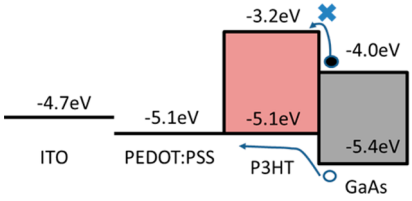

Figure 1. Band alignment of GaAs/P3HT/PEDOT:PSS/ITO.

TABLE 1. Photovoltaic Performances of the Planar Junction of GaAs/P3HT/PEDOT:PSS/ITO

entry	thickness (nm)	passivation	annealing	J_{sc} (mA/cm^2)	fill V_{oc} (V)	fill factor (FF)	η
1	7	no	no	2.77	0.43	30%	0.35%
2		no	yes	3.36	0.45	48%	0.72%
3		yes	no	2.58	0.49	23%	0.29%
4		yes	yes	5.20	0.59	61%	1.86%
5	12	no	no	0.93	0.15	24%	0.03%
6		no	yes	5.10	0.51	38%	1.00%
7		yes	no	6.19	0.61	44%	1.67%
8		yes	yes	6.49	0.61	58%	2.31%
9	15	no	no	0.62	0.15	22%	0.02%
10		no	yes	5.45	0.51	43%	1.20%
11		yes	no	3.09	0.41	25%	0.31%
12		yes	yes	5.24	0.57	49%	1.45%

Prior to applying the polymer on top of GaAs substrates, the surface of GaAs was first passivated. It is generally known that the surface of GaAs contains surface states such as native oxide or dangling bonds, which could quench excited states through nonradiative recombination at the surface and also cause the Fermi level pinning of GaAs. Therefore, a number of chemical passivation methods have been developed, in order to reduce the density of surface states.[27,28] In our study, we adopted a two-step passivation process that first applied 1-octanethiol, followed by ammonium sulfide (see the Experimental Section for details). This two-step process has been found to effectively decrease the surface nonradiative recombination because the ammonium sulfide could further react with remaining sites (on the GaAs) that were unoccupied during the first passivation step with thiols.[27] Next, such passivated GaAs substrates were spin coated with a very thin layer of P3HT with varied thickness (7, 12, or 15 nm), followed by adding the PEDOT:PSS-coated ITO as the anode. For comparative purpose, we also fabricated such devices with unpassivated GaAs (after cleaning with HCl). Finally, half such devices were subjected to thermal annealing at 150 °C for 30 min, since such thermal treatment has been shown to increase the power conversion efficiency of P3HT/fullerene-based organic solar cells due to improved hole

mobility and absorption from the P3HT nanocrystalline phase.[29] All test results, together with fabrication conditions, are listed in Table 1.

A few interesting observations emerge from these results. First, the surface passivation of the GaAs substrates usually offers better results, especially when medium to thick layers of P3HT were applied (*e.g.*, entry 5 *vs* 7, 9 *vs* 11 in Table 1). Second, thermal annealing unanimously leads to a higher efficiency, mainly through much improved J_{sc} when compared with the J_{sc} of these unannealed devices, regardless of the surface passivation (Figure 2a). This indicates that even for such a thin film of P3HT, thermal annealing likely helps improve the morphology of P3HT to benefit a better charge transport. In addition, thermally annealed devices offer slightly higher V_{oc} than those of untreated ones (Figure 2b). Third, Figure 2a shows that J_{sc} begins to plummet once the thickness of P3HT increases over 12 nm. Such a current/thickness dependence for a type II heterojunction-based planar devices is rather unexpected, even taking into account that the exciton diffusion length in P3HT is only less than 10 nm.[30,31] This dependence, however, implies that P3HT in such a planar heterojunction with GaAs might function merely as a hole transport layer and electron blocking layer. In fact, P3HT has been successfully used as a HTL/EBL in GaAs nanowire/PEDOT:PSS hybrid cells[22] and silicon/organic hybrid heterojunction cells.[7]

To gain further insights on photovoltaic behaviors of our GaAs/P3HT planar junctions, we measured the IPCE of devices that showed high efficiencies. Two representative spectra are overlaid in Figure 2c, which shows that the improvement of the photocurrent for the passivated GaAs substrate mainly locates at short wavelengths (*i.e.*, photons with high energy). This is because the photons of high energy—usually having short absorption depth—are much more likely to be affected by the surface states. This additional surface passivation can help reduce the number of these surface states and thereby attenuate the recombination, leaving a higher photon to current conversion (especially in the short-wavelength region). It should also be noted that this passivation can also introduce a surface dipole moment at the GaAs surface. The dipole will have a large effect on the band bending and carrier transport at the organic/inorganic interface,[32] which can also help improve the IPCE.

GaAs/Other Polymers. One important signature for a type II heterojunction is that the open-circuit voltage (V_{oc}) of such a junction would depend upon the energy level difference between the HOMO level/valence band of the p-type semiconductor and the LUMO level/conduction band of the n-type semiconductor. This correlation ($V_{oc} \approx$ energy level difference) has been extensively verified, for example, in polymer/fullerene-based solar cells.[33] For the p-type polymer/n-type GaAs heterojunction, one would expect the V_{oc} should vary with the HOMO level of the polymers

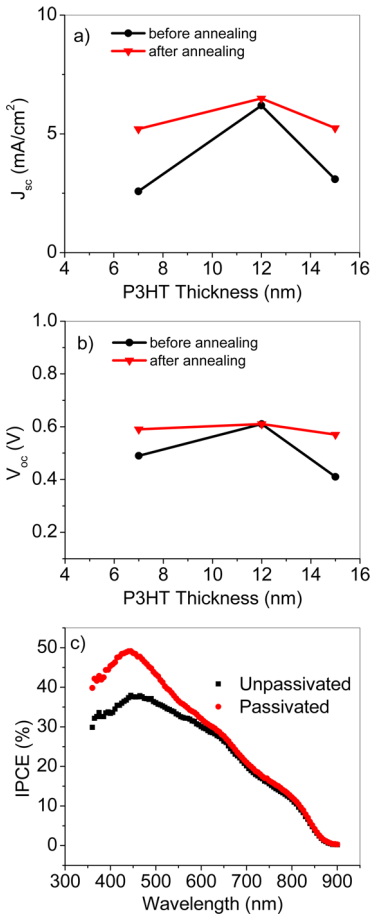

Figure 2. Dependence of (a) J_{sc} and (b) V_{oc} on the thickness of P3HT; (c) effect of passivation on IPCE of ITO/PEDOT:PSS/P3HT (12 nm)/GaAs(100). IPCE data were acquired from devices corresponding to entry 6 and 8 of Table 1. Both devices were annealed.

(since the conduction band of n-type GaAs is fixed). Unfortunately, this important correlation has never been studied for GaAs/polymer junctions: all existing reports exclusively used thiophene-based oligomers or polymers with similar HOMO energy levels. Therefore, after we established a standard device fabrication protocol (*e.g.*, passivation and thermal annealing) through our model study with P3HT, we carefully chose a set of polymers with different HOMO energy levels and band gaps, to further investigate the function of polymers in such heterojunctions.

These selected polymers include poly(9,9-dioctylfluorene-*alt*-benzothiadiazole) (F8BT),[34] poly(benzodithiophene-dithienyldifluorobenzothiadiazole) (PBnDT-DTffBT),[35] and poly(naphthalenedithiophene-dithienyldifluorobenzothiadiazole) (PNDT-DTffBT)[36] (their chemical structures are shown in Figure S1 of the Supporting Information). On the basis of their energy levels and band gaps, these polymers would form different band alignment in regard to the n-type GaAs, as shown in Figure 3. All these GaAs/polymer-based planar heterojunctions were fabricated with the same optimized condition in our model study with GaAs/P3HT, including the

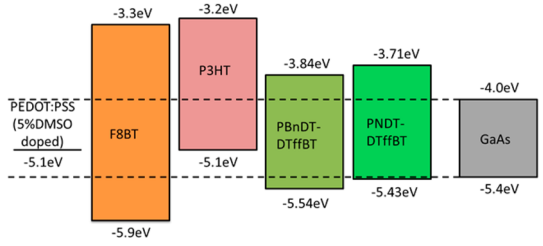

Figure 3. Band alignment of PEDOT:PSS/polymers/GaAs(100) solar cells.

TABLE 2. Photovoltaic Performance of ITO/PEDOT:PSS/PBnDT-DTffBT/Passivated GaAs(100)

thickness (nm)	J_{sc} (mA/cm^2)	V_{oc} (V)	FF	η
5	3.62	0.61	47%	1.04%
10	6.20	0.65	42%	1.68%
14	5.44	0.61	29%	0.98%

TABLE 3. Photovoltaic Performance of ITO/PEDOT:PSS/PNDT-DTffBT/Passivated GaAs(100)

thickness (nm)	J_{sc} (mA/cm^2)	V_{oc} (V)	FF	η
5	1.40	0.61	51%	0.43%
10	6.86	0.65	62%	2.75%
15	4.81	0.65	52%	1.63%

TABLE 4. Photovoltaic Performance of ITO/PEDOT:PSS/F8BT/Passivated GaAs(100)

thickness (nm)	J_{sc} (mA/cm^2)	V_{oc} (V)	FF	η
6	1.91	0.53	23%	0.23%
11	0.30	0.49	27%	0.04%
15	0.19	0.45	36%	0.03%

two-step passivation and thermal annealing. Similarly, three different thicknesses (~5, 10, and 15 nm) were investigated. All tested results are listed in Table 2, Table 3, and Table 4 for PBnDT-DTffBT, PNDT-DTffBT, and F8BT, respectively.

The most striking observation is that the obtained values of V_{oc} for PNDT-DTffBT and PBnDT-DTffBT are very similar to that of P3HT (~0.6 V), although the HOMO energy levels of these polymers vary as much as 0.4 eV (from −5.54 to −5.1 eV). This insensitivity of V_{oc} to HOMO energy levels of these polymers (Figure 4a) cannot be explained by the assumed type II heterojunction, since the V_{oc} of a type II heterojunction should be largely affected by the difference between the conduction band of GaAs and the HOMO of the polymer. It, however, can be predicted by another hypothesis that these polymers simply serve as HTL (and/or EBL) in between the conducting electrode and semiconducting GaAs (a Schottky barrier). F8BT, on the other hand, forms a type I heterojunction with GaAs; therefore little photovoltaic effect was observed (*e.g.*, a

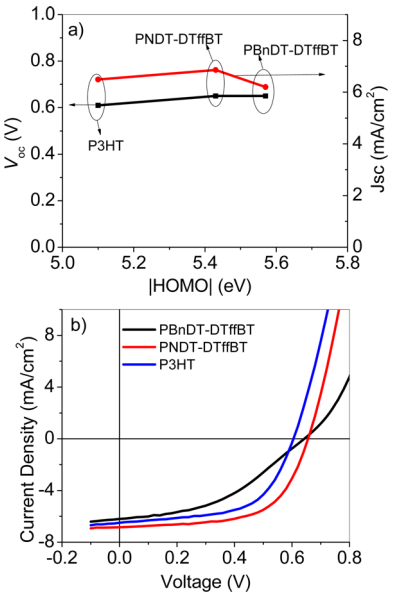

Figure 4. (a) Dependence of V_{oc} and J_{sc} on the HOMO energy level of different polymers; (b) complete $J-V$ curves for optimized devices with different polymers under 1 sun condition (AM 1.5G, 100 mW/cm^2). All data were acquired from devices corresponding to entry 8 of Table 1, and 10 nm thickness entry of Table 2 and Table 3.

very small photocurrent), which was also reported just recently.[37]

With the new hypothesis in mind, the dependence of J_{sc} on the thickness of the polymer for PNDT-DTffBT- and PBnDT-DTffBT-based heterojunctions should be similar to what we observed for the GaAs/P3HT junction, since all these polymers would serve the same function as HTL/EBL. Indeed, the J_{sc} either decreases or levels off after the thickness of polymers surpasses 10 nm (Table 2 and Table 3). Additionally, with a similar thickness of ~10 nm, the value of J_{sc} obtained from the PBnDT-DTffBT-based junction is smaller than those from PNDT-DTffBT- and P3HT-based ones. This can be ascribed to the deeper HOMO energy level of PBnDT-DTffBT (−5.54 eV), which is lower than the valence band of GaAs (−5.4 eV) and thereby can impede the photogenerated holes.

Additional evidence to support our new hypothesis of these polymers functioning as HTL/EBL is provided by the IPCE measurement. As HTL/EBL, these polymers should contribute negligibly to the photocurrent. Additionally, the absorption from the ultrathin layer of polymers is quite small. Therefore, the IPCE spectra from various GaAs/polymer junctions should be dominated by the photoresponse from the GaAs. This was experimentally verified as shown in Figure 5. It should also be noted that the band gap of polymers we used is larger than the band gap of GaAs (~1.4 eV). In this situation, this thin layer of polymers will absorb some photons of high energy. Furthermore, this thin layer of polymers can cause a change of reflection spectrum of the hybrid device. These two effects could lead to the peak shift in the IPCE spectrum.

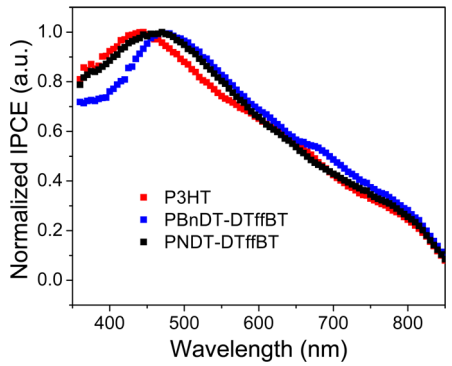

Figure 5. Normalized IPCE spectra of hybrid devices incorporating different active polymers: P3HT, PNDT-DTffBT, and PBnDT-DTffBT.

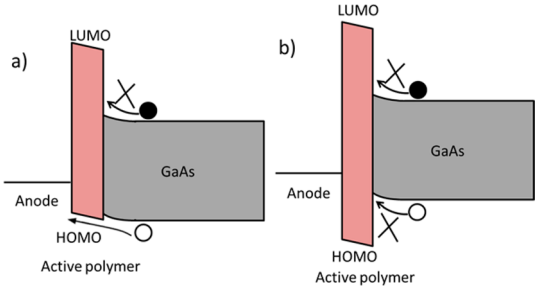

Figure 6. Proposed Schottky junction in GaAs/polymer hybrid solar cell; the role of polymer depends upon the relative position of energy levels with regard to those of GaAs. (a) Polymer serves as HTL/EBL; (b) polymer blocks both electrons and holes.

Proposed Mechanism: Schottky Junction. All these experimental results and related analyses point to a revised working mechanism for such polymer/n-type GaAs planar junctions (Figure 6). Instead of a type II heterojunction between the polymer and the n-type GaAs, a Schottky barrier exists between the n-type GaAs and the anode, while the polymer with appropriate energy levels functions as a HTL/EBL. As schematically shown in Figure 6, the electrons can be blocked by the high LUMO level of the polymer, as in the case for all the polymers we used. If the HOMO level of the polymer is similar to or higher than the valence band of n-type GaAs (−5.4 eV), for example, in the case of PNDT-DTffBT and P3HT, the hole transport is not affected, as shown in Figure 6a. Therefore such a hybrid solar cell will have similarly improved V_{oc} and J_{sc}, regardless of the polymers used (*e.g.*, Figure 4a). In fact, such a Schottky barrier type junction with a blocking layer has already been used in Si/polymer hybrid solar[7] and in GaAs nanowire-based hybrid solar cells.[22] On the other hand, if the HOMO level of the polymer is very deep, as in the case of F8BT, both electron and hole would be blocked by this polymer (Figure 6b). This scenario essentially leads to a type I heterojunction, with a significantly diminished photovoltaic effect (if any).

This proposed Schottky barrier between n-GaAs and anode with polymers as HTL/EBL has an important implication: removing this layer of semiconducting polymer while only keeping the conducting PEDOT:PSS should still offer a working device with a similar V_{oc} to those demonstrated by devices incorporating semiconducting polymers as HTL/EBL (Figure 7). Indeed, such a device, fabricated with the same passivation and thermal annealing condition, offered a V_{oc} value of 0.51 V, slightly lower than the V_{oc} of ~0.6 V demonstrated by the devices with polymer as HTL/EBL. This GaAs/PEDOT:PSS device also showed a higher J_{sc} than those demonstrated earlier. This is because PEDOT:PSS has a work function of *ca.* −5.1 eV and negligible absorption in the region where GaAs absorbs. Thus a better absorption by the GaAs substrate leads to a higher J_{sc}. However, without the polymers as the EBL, this GaAs/EDOT:PSS device would have significant electron recombination at the anode, thereby leading to a smaller V_{oc}. All data are tabulated in Table 5, together with the results of devices with unpassivated GaAs. Again, passivation of the GaAs is beneficial to the device performance, as we observed earlier.

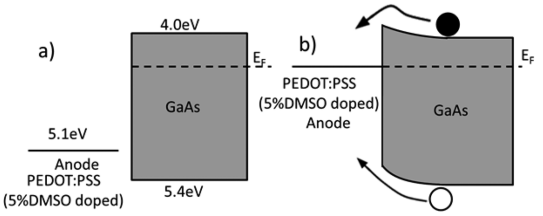

Figure 7. Band structure of a Schottky junction solar cell of ITO/PEDOT:PSS/GaAs (a) before and (b) after Fermi level alignment.

TABLE 5. Photovoltaic Performance of ITO/PEDOT:PSS/GaAs(100)

	J_{sc} (mA/cm^2)	V_{oc} (V)	FF	η
unpassivated	5.23	0.47	32%	0.78%
passivated	7.74	0.51	48%	1.91%

Schottky Barrier Height. To shed more light on the proposed Schottky barrier between n-GaAs and anode with polymers as HTL/EBL, we calculated the Schottky barrier height. Assuming the anode and n-GaAs form a Schottky diode, the current−voltage measurement of such diodes offers a convenient method to determine the Schottky barrier height. First, the fitting of dark currents measured from all devices (Figure S2) to the modified Shockley equation with series resistance and parallel resistance offers the ideality factor and saturated current in the Schottky junction. Then the barrier height can be obtained from the saturated current according to eq 1:

$$\Phi_B = \frac{kT}{q}\ln\left(\frac{A^{**}T^2}{J_s}\right) \quad (1)$$

where q is the absolute electronic charge, Φ_B is the Schottky barrier height, J_s is the saturated current, k is

TABLE 6. Fitting Results of Devices with ~10 nm Polymer as Blocking Layer

polymer	R_s ($\Omega \cdot cm^2$)	R_p ($\Omega \cdot cm^2$)	J_s (mA/cm^2)	n	Φ_B (eV)
P3HT	7.2	7.61×10^2	5.11×10^{-9}	1.15	1.18
PNDT-DTffBT	6.4	4.72×10^3	1.83×10^{-10}	1.08	1.27
PBnDT-DTffBT	8.8	2.72×10^5	2.49×10^{-9}	1.38	1.20
F8BT	24.7	1.36×10^5	1.13×10^{-8}	1.47	1.16
NA (PEDOT only)	5.0	6.52×10^2	5.68×10^{-7}	1.40	1.06

Boltzmann's constant, T is the absolute temperature, A^{**} is the effective Richardson constant (for n-GaAs, A^{**} = 4.4 A/(cm^2 K^2)).[38]

The fitting results are listed in Table 6 (details regarding fitting and calculation are described in the Supporting Information). First, the Schottky barrier height for all polymer/GaAs-based devices is ~1.2 eV, regardless of the band gap and energy levels of the polymer used. This is a direct evidence to support the proposed Schottky junction. A slightly lower barrier height was obtained for the PEDOT:PSS-only device without the polymer blocking layer. Second, the ideality factor n, which usually reflects the recombination in the device, gradually increases from ~1.1 for P3HT- and PNDT-DTffBT-based devices to ~1.4 for PBnDT-DTffBT- and F8BT-based ones. This is because P3HT/PNDT-DTffBT can block only electron from n-GaAs, while the PBnDT-DTffBT/F8BT can block both electron and hole from n-GaAs, increasing the probability of charge recombination and thereby the ideality factor. This observation is also well consistent with the photovoltaic performance of these polymer/GaAs-based devices.

Additional evidence for the proposed Schottky junction in the GaAs/polymer hybrid solar cell was obtained through investigating the change of Schottky barrier height by varying the work function of the metal used as the anode in our devices. Experimentally, we switched the PEDOT:PSS in the device to two other metals of noticeably different work functions (Al of 4.3 eV and Au of 5.1 eV). These metals were thermally evaporated on top of the n-GaAs, with or without P3HT, as thin layer (~15 nm) to allow the light absorption by n-GaAs to show the photovoltaic effect. The measured $J-V$ curves under light (1 sun AM 1.5 condition) and in the dark are displayed in the Supporting Information (Figures S3 and S4), with photovoltaic parameters listed in Table S6 and parameters fitted from the dark current listed in Table S7. In theory, a Schottky junction would predict that the barrier height should change as the work function of the metal varies, if no strong Fermi level pinning is present. With Fermi level pinning due to a significant amount of surface states on n-GaAs, the Schottky barrier height would be fixed to 0.8−0.9 eV for n-GaAs in the gas phase, *independent* of the work function of the metal. However, Fermi level pinning, as a surface effect, is sensitive to the method of preparing the surface. Any surface treating methods, such as chemical etching or passivation, would reduce the amount of these surface states and thereby suppress the Fermi level "pinning". In this scenario, the Schottky barrier height would still be affected by the metal work function, though not as much as one would expect from a Schottky barrier without any Fermi level pinning.[39,40] This is why we observed only a slight increase in the barrier height (0.15−0.25 eV) when we switched from Al to Au, though Au has a much higher work functions than that of Al (~0.8 eV). Nevertheless, the work function-dependent barrier height also supports the junction of anode/polymer (about 10 nm)/GaAs is a Schottky barrier type junction.

CONCLUSION

Through our systematic investigation of polymer/n-type GaAs heterojunctions, including semiconducting conjugated polymers of different band gap and energy levels, with optimized device fabrication conditions, we reach the following conclusions. First of all, a polymer/n-type GaAs planar junction based solar cell is *not* a type II heterojunction as originally assumed. Instead, n-type GaAs forms a Schottky barrier with its corresponding anode, while the semiconducting polymer of appropriate energy levels can function as HTL/EBL. Because of this, only an ultrathin layer of polymer (~10 nm) is necessary. Second, as many have shown, passivating the surface of GaAs does help improve the performance of such devices. Third, annealing of our polymer/n-GaAs planar junctions also offers improvement on the device characteristics, although the exact mechanism still needs further study. Finally, please note that our conclusions are limited to the (100) n-type GaAs. Different results can and will emerge when switching to different orientations and types of GaAs.[24,37] Additionally, nanostructured devices with increased surface area and a possible light-trapping effect can certainly boost the efficiency, especially the current.[22,25]

EXPERIMENTAL SECTION

A Si-doped n-type (100) GaAs wafer with carrier concentration of 1×10^{18} cm^{-3} from Wafer Technology Ltd. with annealed AuGe/Ni/Au back ohmic contact was cleaned by dipping in acetone and 2-propanol sequentially for 5 min each. Then the GaAs wafer was immersed in aqueous HCl (10% v/v) solution for 30 s to remove the native oxide. After that, the GaAs wafer for passivation was immersed in a 30 mM ethanolic solution of 1-octanethiol for 5 h and then further passivated by a 22 wt % aqueous ammonium sulfide solution for 15 min. Such a passivated GaAs wafer was then transferred into a nitrogen-filled glovebox (MBraun USA, Inc.). The active polymers were dissolved in *o*-dichlorobenzene at a given concentration and stirred at 120 °C overnight in the nitrogen-filled glovebox. The hot polymer solution was then spin coated on top of the passivated or unpassivated GaAs wafer at 1700 rpm

for 1 min, and this GaAs/polymer heterojunction was kept in a sealed Petri dish overnight. The as-formed GaAs/polymer junction was then taken out of the glovebox and spin coated with 5% DMSO-doped PEDOT:PSS (Clevios PH500) with Zonyl FSO-100 surfactant (Sigma-Aldrich, 5 mg of Zonyl FSO-100 in 1 mL of doped PEDOT:PSS) at 2500 rpm for 1 min to get a thin PEDOT:PSS layer on top of the GaAs/polymer substrate. In the meantime, a separate ITO glass was cleaned by ultrasonication in deionized water, acetone, and 2-propanol sequentially for 15 min each and then dried under a stream of nitrogen and subjected to treatment with UV-ozone for 15 min. The DMSO-doped PEDOT:PSS was also spin coated on top of the cleaned ITO glass at 1200 rpm for 10 s. Then the previously fabricated PEDOT:PSS/polymer/GaAs substrate was put face down on top of the ITO substrate when the PEDOT:PSS layer on ITO glass was still wet. The entire device (ITO/PEDOT:PSS/polymer/GaAs/cathode) was then transferred into a vacuum oven and left to dry at room temperature for 3 h. The optional step of thermal annealing of the entire device was conducted inside the glovebox at 150 °C for 30 min. Finally, the photovoltaic performance characterization of the finished devices was assessed with the solar simulator (Oriel 91160, 300 W) under AM1.5 global one sun (100 mW/cm^2 calibrated by an NREL-certified standard silicon cell) at room temperature in the glovebox. Current density *versus* potential (*J*−*V*) curves were recorded with a Keithley 2400 digital source meter. The incident photon-to-current conversion efficiency measurement was carried out under monochromatic illumination (Oriel Cornerstone 260 1/4 m monochromator equipped with an Oriel 70613NS QTH lamp), and the calibration of the incident light was performed with a monocrystalline silicon diode. The active area was calculated by photograph of the whole area of the GaAs wafer. The film thickness was measured by a profilometer (Alpha-Step D-100 Stylus Profiler, KLA-Tencor) and calibrated by an ellipsometer (J. A. Woollam VASE).

Conflict of Interest: The authors declare no competing financial interest.

Supporting Information Available: The chemical structures of all polymers, *J*−*V* curves in the dark, details of fitting of dark current curves, and detailed photovoltaic performance for the optimized devices for each active polymer are included. This material is available free of charge *via* the Internet at http://pubs.acs.org.

Acknowledgment. We acknowledge support from an NSF SOLAR Grant (DMR-1125803) and Prof. Huffaker and Ramesh B. Laghumavarapu of UCLA for GaAs substrates with back metal contact.

REFERENCES AND NOTES

1. Moulé, A. J.; Chang, L.; Thambidurai, C.; Vidu, R.; Stroeve, P. Hybrid Solar Cells: Basic Principles and the Role of Ligands. *J. Mater. Chem.* **2012**, *22*, 2351.
2. Tang, A.; Qu, S.; Teng, F.; Hou, Y.; Wang, Y.; Wang, Z. Recent Developments of Hybrid Nanocrystal/Polymer Bulk Heterojunction Solar Cells. *J. Nanosci. Nanotechnol.* **2011**, *11*, 9384–9394.
3. Zhao, L.; Lin, Z. Crafting Semiconductor Organic-Inorganic Nanocomposites *via* Placing Conjugated Polymers in Intimate Contact with Nanocrystals for Hybrid Solar Cells. *Adv. Mater.* **2012**, 4353–4368.
4. Shen, X.; Sun, B.; Liu, D.; Lee, S.-T. Hybrid Heterojunction Solar Cell Based on Organic-Inorganic Silicon Nanowire Array Architecture. *J. Am. Chem. Soc.* **2011**, *133*, 19408–19415.
5. Lu, W.; Wang, C.; Yue, W.; Chen, L. Si/PEDOT:PSS Core/Shell Nanowire Arrays for Efficient Hybrid Solar Cells. *Nanoscale* **2011**, *3*, 3631–3634.
6. Syu, H.-J.; Shiu, S.-C.; Lin, C.-F. Silicon Nanowire/Organic Hybrid Solar Cell with Efficiency of 8.40%. *Sol. Energy Mater. Sol. Cells* **2012**, *98*, 267–272.
7. Avasthi, S.; Lee, S.; Loo, Y.-L.; Sturm, J. C. Role of Majority and Minority Carrier Barriers Silicon/Organic Hybrid Heterojunction Solar Cells. *Adv. Mater.* **2011**, *23*, 5762–5766.
8. Lu, W.; Chen, Q.; Wang, B.; Chen, L. Structure Dependence in Hybrid Si Nanowire/Poly(3,4-ethylenedioxythiophene): Poly(styrenesulfonate) Solar Cells: Understanding Photovoltaic Conversion in Nanowire Radial Junctions. *Appl. Phys. Lett.* **2012**, *100*, 023112.
9. Conings, B.; Baeten, L.; Boyen, H.-G.; Spoltore, D.; D'Haen, J.; Van Bael, M. K.; Manca, J. V. Generalized Approach to the Description of Recombination Kinetics in Bulk Heterojunction Solar Cells—Extending from Fully Organic to Hybrid Solar Cells. *Appl. Phys. Lett.* **2012**, *100*, 203905.
10. AbdulAlmohsin, S.; Cui, J. B. Graphene-Enriched P3HT and Porphyrin-Modified ZnO Nanowire Arrays for Hybrid Solar Cell Applications. *J. Phys. Chem. C* **2012**, *116*, 9433–9438.
11. Yang, J.; Qian, L.; Zhou, R.; Zheng, Y.; Tang, A.; Holloway, P. H.; Xue, J. Hybrid Polymer:Colloidal Nanoparticle Photovoltaic Cells Incorporating a Solution-Processed, Multifunctioned ZnO Nanocrystal Layer. *J. Appl. Phys.* **2012**, *111*, 044323.
12. Liao, W.-P.; Hsu, S.-C.; Lin, W.-H.; Wu, J.-J. Hierarchical TiO_2 Nanostructured Array/P3HT Hybrid Solar Cells with Interfacial Modification. *J. Phys. Chem. C* **2012**, *116*, 15938–15945.
13. Tai, Q.; Zhao, X.; Yan, F. Hybrid Solar Cells Based on Poly(3-hexylthiophene) and Electrospun TiO_2 Nanofibers with Effective Interface Modification. *J. Mater. Chem.* **2010**, *20*, 7366–7371.
14. Liao, H.-C.; Lee, C.-H.; Ho, Y.-C.; Jao, M.-H.; Tsai, C.-M.; Chuang, C.-M.; Shyue, J.-J.; Chen, Y.-F.; Su, W.-F. Diketopyrrolopyrrole-Based Oligomer Modified TiO_2 Nanorods for Air-Stable and All Solution Processed Poly(3-hexylthiophene): TiO_2 Bulk Heterojunction Inverted Solar Cell. *J. Mater. Chem.* **2012**, *22*, 10589.
15. Liu, Q.; Ono, M.; Tang, Z.; Ishikawa, R.; Ueno, K.; Shirai, H. Highly Efficient Crystalline Silicon/Zonyl Fluorosurfactant-Treated Organic Heterojunction Solar Cells. *Appl. Phys. Lett.* **2012**, *100*, 183901.
16. Blakemore, J. S. Semiconducting and Other Major Properties of Gallium Arsenide. *J. Appl. Phys.* **1982**, *53*, R123.
17. Casey, H. C.; Sell, D. D.; Wecht, K. W. Concentration Dependence of the Absorption Coefficient for n- and p-Type GaAs between 1.3 and 1.6 eV. *J. Appl. Phys.* **1975**, *46*, 250–257.
18. Green, M. A.; Emery, K.; Hishikawa, Y.; Warta, W.; Dunlop, E. D. Solar Cell Efficiency Tables (Version 39). *Prog. Photovoltaics Res. Appl.* **2012**, *20*, 12–20.
19. Horowitz, G.; Garnier, F. Polythiophene-GaAs p-n Heterojunction Solar Cells. *Solar Energy Mater.* **1986**, *13*, 47–55.
20. Ackermann, J.; Videlot, C.; El Kassmi, A.; Guglielmetti, R.; Fages, F. Highly Efficient Hybrid Solar Cells Based on an Octithiophene-GaAs Heterojunction. *Adv. Funct. Mater.* **2005**, *15*, 810–817.
21. Bi, H.; Lapierre, R. R. A GaAs Nanowire/P3HT Hybrid Photovoltaic Device. *Nanotechnology* **2009**, *20*, 465205.
22. Chao, J.-J.; Shiu, S.-C.; Lin, C.-F. GaAs Nanowire/Poly(3,4-ethylenedioxythiophene):Poly(styrenesulfonate) Hybrid Solar Cells with Incorporating Electron Blocking Poly(3-hexylthiophene) Layer. *Sol. Energy Mater. Sol. Cells* **2012**, *105*, 40–45.
23. Chao, J.-J.; Shiu, S.-C.; Hung, S.-C.; Lin, C.-F. GaAs Nanowire/Poly(3,4-ethylenedioxythiophene):Poly(styrenesulfonate) Hybrid Solar Cells. *Nanotechnology* **2010**, *21*, 285203.
24. Ren, S.; Zhao, N.; Crawford, S. C.; Tambe, M.; Bulović, V.; Gradecak, S.; Bulović, V.; Gradečak, S. Heterojunction Photovoltaics Using GaAs Nanowires and Conjugated Polymers. *Nano Lett.* **2011**, *11*, 408–413.
25. Mariani, G.; Laghumavarapu, R. B.; Tremolet de Villers, B.; Shapiro, J.; Senanayake, P.; Lin, A.; Schwartz, B. J.; Huffaker, D. L. Hybrid Conjugated Polymer Solar Cells Using Patterned GaAs Nanopillars. *Appl. Phys. Lett.* **2010**, *97*, 013107.
26. Kim, J. Y.; Lee, K.; Coates, N. E.; Moses, D.; Nguyen, T.-q.; Dante, M.; Heeger, A. J. Efficient Tandem Polymer Solar Cells Fabricated by All-Solution Processing. *Science* **2007**, *317*, 222–225.
27. Arudra, P.; Marshall, G. M.; Liu, N.; Dubowski, J. J. Enhanced Photonic Stability of GaAs in Aqueous Electrolyte Using Alkanethiol Self-Assembled Monolayers and Postprocessing with Ammonium Sulfide. *J. Phys. Chem. C* **2012**, *116*, 2891–2895.

28. Jun, Y.; Zhu, X. Y.; Hsu, J. W. P. Formation of Alkanethiol and Alkanedithiol Monolayers on GaAs(001). *Langmuir* **2006**, *22*, 3627–3632.
29. Ma, W.; Yang, C.; Gong, X.; Lee, K.; Heeger, A. J. Thermally Stable, Efficient Polymer Solar Cells with Nanoscale Control of the Interpenetrating Network Morphology. *Adv. Funct. Mater.* **2005**, *15*, 1617–1622.
30. Shaw, P. E.; Ruseckas, A.; Samuel, I. D. W. Exciton Diffusion Measurements in Poly(3-hexylthiophene). *Adv. Mater.* **2008**, *20*, 3516–3520.
31. Goh, C.; Scully, S. R.; McGehee, M. D. Effects of Molecular Interface Modification in Hybrid Organic-Inorganic Photovoltaic Cells. *J. Appl. Phys.* **2007**, *101*, 114503.
32. He, L.; Jiang, C.; Wang, H.; Lai, D.; Rusli High Efficiency Planar Si/Organic Heterojunction Hybrid Solar Cells. *Appl. Phys. Lett.* **2012**, *100*, 073503.
33. Zhou, H.; Yang, L.; You, W. Rational Design of High Performance Conjugated Polymers for Organic Solar Cells. *Macromolecules* **2012**, *45*, 607–632.
34. Chua, L. L.; Zaumseil, J.; Chang, J. F.; Ou, E. C. W. General Observation of n-Type Field-Effect Behaviour in Organic Semiconductors. *Nature* **2005**, *434*, 194–199.
35. Zhou, H.; Yang, L.; Stuart, A. C.; Price, S. C.; Liu, S.; You, W. Development of Fluorinated Benzothiadiazole as a Structural Unit for a Polymer Solar Cell of 7% Efficiency. *Angew. Chem., Int. Ed.* **2011**, *50*, 2995–2998.
36. Yang, L.; Tumbleston, J. R.; Zhou, H.; Ade, H.; You, W. Disentangling the Impact of Side Chains and Fluorine Substituents of Conjugated Donor Polymers on the Performance of Photovoltaic Blends. *Energy Environ. Sci.* **2013**, *6*, 316–326.
37. Yong, C. K.; Noori, K.; Gao, Q.; Joyce, H. J.; Tan, H. H.; Jagadish, C.; Giustino, F.; Johnston, M. B.; Herz, L. M. Strong Carrier Lifetime Enhancement in GaAs Nanowires Coated with Semiconducting Polymer. *Nano Lett.* **2012**, *12*, 6293–6301.
38. Sze, S. M.; Ng, K. K. *Physics of Semiconductor Devices*; John Wiley & Sons, Inc.: New York, 2006.
39. Fan, J.-F.; Oigawa, H.; Nannichi, Y. Metal-Dependent Schottky Barrier Height with the $(NH_4)_2S_x$-Treated GaAs. *Jpn. J. Appl. Phys.* **1988**, *27*, L2125–L2127.
40. Rhoderick, E. H. The Physics of Schottky Barriers. *J. Phys. D: Appl. Phys.* **1970**, *3*, 1153–1167.